Asimetrik Dişlilerde Diş Dibi Gerilmelerinin Hesaplanması için Yeni Bir Yöntem

Oğuz DOĞAN[1*], Celalettin YÜCE[2], Fatih KARPAT[3]

[1]Kahramanmaraş Sütçü İmam Üniversitesi Mühendislik ve Mimarlık Fakültesi Makine Mühendisliği Bölümü Konstrüksiyon ve İmalat Anabilim Dalı, Kahramanmaraş
[2,3] Bursa Uludağ Üniversitesi Mühendislik Fakültesi Makine Mühendisliği Bölümü Konstrüksiyon ve İmalat Anabilim Dalı, Bursa

[1]https://orcid.org/0000-0003-4203-8237
[2]https://orcid.org/0000-0001-5894-8986
[3]https://orcid.org/0000-0001-8474-7328
*Sorumlu yazar: oguzdogan@ksu.edu.tr

ÖZ

Günümüzde asimetrik diş profillerine sahip dişli tasarımları, dişlilerin diş kökü gerilmelerinin azaltılmasında önemli çözümler sunmaktadır. Asimetrik diş profiline sahip dişlilerde diş dibi gerilmelerini hesaplamak için sayısal, analitik ve deneysel çalışmalar yapılmasına rağmen literatürde standart veya basitleştirilmiş bir denklem veya ampirik ifadeye rastlanmamıştır. Bu çalışmada hem DIN3990 standardı hem de sonlu elemanlar yöntemi kullanılarak asimetrik diş profillerine sahip dişliler için yeni bir diş dibi gerilmesi hesaplama prosedürü geliştirilmiştir. Simetrik profilli dişlilerin diş dibi gerilmeleri geliştirilen sonlu elemanlar modeli ile belirlenmiş ve sonuçlar DIN 3990 standardı ile karşılaştırılarak doğrulanmıştır. Doğrulanmış sonlu elemanlar modeli kullanılarak, süren taraf basınç açısı 20° ile 30° arasında ve diş sayısı 18 ile 100 arasında değiştirilerek 66 farklı durum incelenmiş ve asimetrik profile sahip dişlilerdeki diş dibi gerilmeleri belirlenmiştir. Analizler sonucunda yeni bir asimetriklik faktörü elde edilmiştir. Elde edilen faktörün DIN 3390 formülüne eklenmesiyle asimetrik profilli dişlilerin diş dibi gerilmelerinde kullanılmak üzere yeni bir denklem türetilmiştir. Bu denklem sayesinde tasarımcıların, asimetrik diş profiline sahip dişlilerde sonlu elemanlar analizine ihtiyaç duymadan diş dibi gerilmelerini yüksek hassasiyetle hesaplayabilmeleri ön görülmektedir.

A Novel Method for Tooth Bending Stress Calculation of Gears with Asymmetric Teeth

ABSTRACT

Today, gear designs with asymmetric tooth profiles offer essential solutions in reducing tooth root stresses of gears. Although numerical, analytical, and experimental studies are carried out to calculate the bending stresses in gears with asymmetric tooth profiles a standard or a simplified equation or empirical statement has not been encountered in the literature. In this study, a novel bending stress calculation procedure for gears with asymmetric tooth profiles is developed using both the DIN3990 standard and the finite element method. The bending stresses of gears with symmetrical profile were determined by the developed finite element model and was verified by comparing the results with the DIN 3990 standard. Using the verified finite element model, by changing the drive side pressure angle between 20° and 30° and the number of teeth between 18 and 100, 66 different cases were examined and the bending stresses in gears with asymmetric profile were determined. As a result of the analysis, a new asymmetric factor was derived. By adding the obtained asymmetric factor to the DIN 3390 formula, a new equation has been derived to be used in tooth bending stresses of gears with asymmetric profile. Thanks to this equation, it is

anticipated that designers will be able to calculate tooth root stresses with high precision in gears with asymmetric tooth profiles, without the need for finite element analysis.

1. Introduction

Today, increasing sustainability concerns have made gears that provide high-efficiency power transmission a priority target in many industries, especially in the automobile, aviation, and machinery sectors. Research and development on the gear systems focused on meeting the demands of higher load-carrying capacity, weight reduction, and more torque transmission with low-cost gears (He et al., 2021). New gear designs are needed to meet these performance expectations.

Most gears used today have teeth with a symmetric profile. In these gears, since the pressure angle of both surfaces is equal, the contact and bending stresses on both surfaces of the tooth are equal. During transmitting motion or power, gears generally operate in one direction. For this reason, while one side of the tooth, which is called the drive side, is exposed to high loads during its lifetime, there is no loading on the other side of the tooth, which is called the coast side. This situation has led to the design of gears with asymmetric profiles (Kapelevich, 2000). The most important advantage of the asymmetrical profile teeth is that they allow higher torque transmission by reducing the contact stress on the drive side (Karpat et al., 2008). Another significant advantage is that the tooth stiffness can be controlled by designing the drive side pressure angle (DSPA) different from the coast side. In this way, the vibration and noise of the gear pair working together are reduced (Litvin et al., 2000). Due to these advantages, the use of involute spur gears with an asymmetric profile is rapidly increasing, especially in areas with high-performance expectations.

During the torque transfer, high stresses, especially at the local contact line and root regions of the involute gears, cause fracture damage. These stresses in the root area, called bending stresses, are critical performance indicators for gear designers as they cause damage and loss of performance (Wen et al., 2018). Bending stresses can be calculated analytically using standard parameters for gears with symmetric profiles with the help of norms such as ISO 6336-1:2019 (ISO 6336, 2002), ANSI/AGMA 2001- D04 (Drago, 1982) and DIN 3990 (DIN 3990, 1987). However, the previously mentioned standard calculation methods are not valid, as maximum stress does not occur at the 30° tangent of the root fillet in teeth with asymmetrical profiles. These methods differ somewhat in the techniques used to establish the gear geometry required for this calculation and their stress concentration factors (Lisle et al., 2017). Today, experimental methods have been used to determine the bending stresses (Costopoulos et al., 2016; Dharashivkar et al., 2016; Karpat et al., 2020) impact stress (Kalay et al., 2020) and fatigue properties (Demet et al., 2018) of gears with asymmetrical profiles. However, these methods find limited application areas due to their long duration and high costs. The most important problem experienced in measuring root stress with experimental methods is the error in the positional accuracy of the gauge, especially in small modulus gears (Lisle et al., 2017). Therefore, many researchers have carried out

analytical studies on the stress analysis of gears with asymmetrical profiles in recent years. Although some results can be obtained with analytical methods, it is not possible to obtain exact results due to the complex geometries of the gears and the coefficients used in the calculations. For this reason, the finite element method (FEM) has started to be used by many researchers in the calculation of tooth bending stress. Cavdar et al., (2005) examined the bending stresses and contact ratio depending on the DSPA by adapting the DIN 3990 and ISO 6336-1:2019 norms to the asymmetric tooth profile. They stated that with the increase of the DSPA, the bending load capacity increased while the bending stress decreased. Spitas et al., (2007) optimized the tooth geometry to achieve minimum tooth root stress in non-standard involute gears. The optimized tooth design achieved an 8.5% reduction in root stress and confirmed this result experimentally.

Karpat et al., (2005) and Di Francesco and Marini (2007) have developed several computer programs to optimize the tooth design to achieve maximum performance from asymmetric gear. Costopoulos et al., (2009) have achieved a 28% increase in load-carrying capacity with their asymmetric gear designs than teeth with a symmetric profile. Karpat et al., (2014) performed finite element analysis (FEA) using a 2D tooth model to calculate tooth stiffness for dynamic analysis depending on the DSPA and the number of teeth. Pedersen, (2010) showed that the bending stress was reduced with the optimized asymmetric gear design obtained by changing the tool geometry. Pramono and Rizal (2021) developed FE model to investigate the effects of the asymmetric factor on dynamic bending stress variation of the spur gears. The DSPA was altered 22.77° to 26.31° in the FE analysis. The bending stress was decreased considerably when the asymmetric factor was increased 1 to 1.08. Senthil Kumar et al. (2008) investigated the influence of pressure angle, asymmetric factors, and profile shift on the maximum fillet stress to propose the optimum parameter levels that improve the fillet bending capacity. They also compared the FEA model results they used in their studies with ISO 6336-1:2019 and ANSI/AGMA 2001- D04 standards for symmetric gears. Keçici et al., (2021) investigated the effect of DSPA on gear performances. It was observed that the load bearing capacity, performance, life, efficiency and reliability increased by using the asymmetric profile. Yılmaz et al., (2022) performed numerical analyzes to determine bending stress and dynamic behavior of the hybrid spur gears with asymmetric teeth. The bending stress values were decreased approximately 9% when the DSPA was increased 20° to 30°. However, the dynamic factor of the hybrid spur gears was increased 1.45 to 1.8. Sekar et al., (2015) determined the tooth form factor for asymmetric gears with different DSPA and Coast side pressure angles (CSPA) with the ISO 6336-1:2019 standard. They adapted using FEM. Marimuthu et al., (2016) also adopted a FEM to compare directly designed symmetrical and asymmetrical high contact ratio (HCR) spur gears and traditional symmetrical HCR spur gears for their load-carrying capacity. Lisle et al., (2006) compared the root bending stress of spur gear calculated by ISO, AGMA and FEA methods with the experimental results and stated that more accurate results can be obtained with FEA. Thomas et al., (2018) applied a search method to calculate the bending stress of asymmetric spur gear, and they compared the results with ISO 6336-1:2019 and FEA methods. They propose a new method and

coordinate system for the calculation of the bending stress of spur gears with asymmetric teeth analytically.

In the literature review, it was seen that, although there are standards based on analytical methods to determine the bending stresses of gears with symmetric profiles, a standard is not available for gears with asymmetric teeth profiles. Experimental and numerical studies have been carried out to determine the bending stresses of gears with asymmetric teeth. However, the lack of a simplified equation or empirical statement that will allow gear designers to get to the conclusion faster is a significant drawback. As well as, although FEA can be incredibly accurate, it requires no gear expertise and can produce wrong and misleading results often as a consequence of over simplified gear models, incorrect boundary conditions and poor mesh quality.

This study proposes a novel bending stress calculation method based on DIN 3990 / Method C and FEA analysis for gear with asymmetric teeth. The effects of DSPA and tooth number on the bending stress are evaluated numerically. A novel bending stress calculation factor called the asymmetry factor is proposed using the maximum bending root stress results from the FEA. The maximum root bending stress can be easily calculated using the proposed asymmetry factor and DIN 3990 / Method C standard for gears with asymmetric teeth. The asymmetry factor has simplified the calculation of the gear root bending stress. The stress values can be analytically calculated by using this factor, without any numerical or experimental study.

2. Material and Method

2.1. Creation of the Gear Geometry

In this study, gear geometries were created by mathematical modeling based on Litvin's vector method. In this method, firstly, the equations and limits of the rack cutter tool, which manufactured the gears, are determined. Then the spur gear geometry is created using the coordinate transformation, differential geometry, and gear theory. The geometry of the rack type cutting tool is seen in Figure 1. In this geometry, the ac – bd zones shape the bottom region of the gear; the ce – df zones shape the trochoid zone of the gear, and the eg – fh zones shape the involute zone of the gear wheel. O (X, Y) is positioned in the middle of the space width. More detail about the creation of the gear geometries is given in (Dogan et al., 2018).
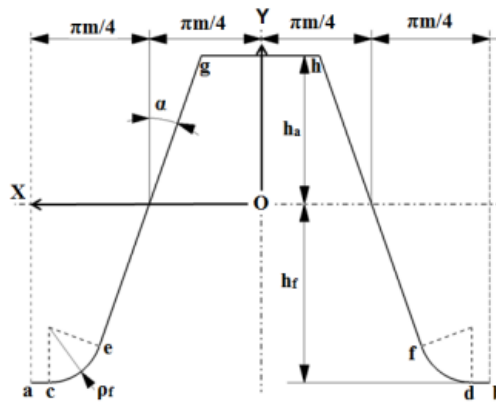
Figure 1. The geometry of the rack type cutter tool

2.2. Calculation of Tooth Bending Stress via DIN3990

In the literature, different standards have been developed so far to calculate bending stress in involute spur gears with symmetric teeth. Among them, ISO 6336-1:2019 (ISO 6336, 2002) and DIN 3990 (DIN 3990, 1987) standards are the most widely used. Although they are similar to each other, there are some minor differences. With these standards, the following assumptions are used in the calculation of tooth bending stress;

• The critical section of the tooth is the thickness of the point tangent to the tooth root at an angle of 30°, starting from the axis of tooth symmetry, as shown in Figure 2.

• The compressive stress caused by the radial component of the normal force on the gear is negligible.

• In DIN 3990 / Method C and ISO 6336-1:2019, the tooth load is assumed to effect on the tip of the teeth.

In this study, the calculations were done according to the DIN 3990 / Method C. So, the force was applied to the addendum circle of the teeth.
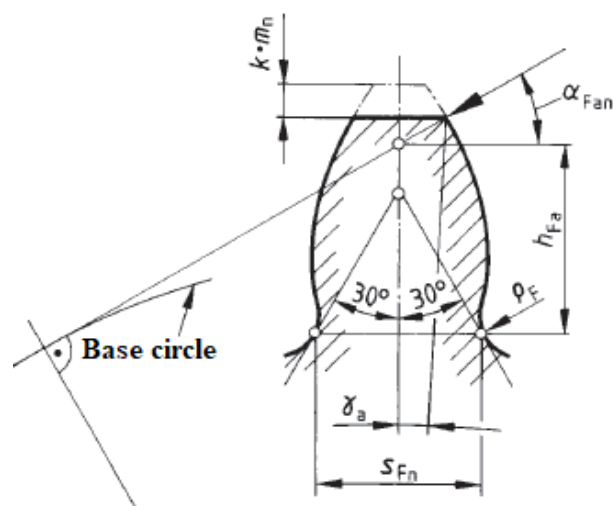
Figure 2. Tooth model for bending stress DIN 3990 / Method C (DIN 3990, 1987)

According to the DIN 3990 / Method C, the maximum tooth root stress can be calculated by using the following equations.

$$\sigma_{F0-C} = \frac{F_t}{b\,m_n} Y_{Fa}\,Y_{Sa}\,Y_\varepsilon\,Y_\beta \tag{1}$$

$$F_t = F\cos\alpha \tag{2}$$

Where; F_t tangential gear force, b tooth width, m_n is defined as a normal module.

Y_{Fa} tooth form factor can be defined as,

$$Y_{Fa} = \frac{6\,(h_{Fa}/m_n)}{(S_{Fn}/m_n)^2}\frac{\cos\alpha_{Fan}}{\cos a_n} \tag{3}$$

Y_{Sa} stress concentration factor can be defined as,

$$Y_{Sa} = \left(1.2 + 0.13\,\frac{S_{Fn}}{h_{Fa}}\right)\left(\frac{S_{Fn}}{2\rho_F}\right)^{1/[1.21+2.3\,(h_{Fa}/S_{Fn})]} \tag{4}$$

Y_ε load sharing factor (Contact factor) can be calculated via the following equation.

$$Y_\varepsilon = 0.25 + {0.75}/{\varepsilon_\alpha} \tag{5}$$

Where, ε_α is the contact ratio of the spur gear pair and can be calculated as:

$$\varepsilon_\alpha = \frac{\sqrt{r_{a1}^2 - r_{b1}^2} + \sqrt{r_{a2}^2 - r_{b2}^2} - a_d\sin\alpha_d}{p\cos\alpha_d} \tag{6}$$

Where, r_{a1}, r_{b1}, r_{a2}, r_{b2} addendum and base circles of the pinion and gear, a_d is the distance between axes, α_d is the drive side pressure angle, p is pitch.

In this study, bending stress was calculated on a single tooth using the finite element method. Therefore, some assumptions have been made. The load sharing factor (Y_ε) was not considered in the calculations. The single tooth load was applied to the tip of the tooth and since the helix angle is zero on spur gears the helix factor Y_β is determined as 1. Form factor (Y_{Fa}) and stress concentration factor (Y_{Sa}) values are changed depending on the several parameters such as tool geometry, addendum, dedendum, tooth number, profile shifting factor, rack cutter tip radius, etc. In the well-known standards such as DIN 3990 and ISO 6336-1:2019, many graphics or tables are required to get these factors. According to the DIN 3990 standard, for the rack cutter tip radius (ρ_F) of 0.3m, the variation of the Y_{Fa} and Y_{Sa} is given in Figure 3. Moreover, these coefficients can be calculated by using the above equations. The equations are more suitable for computer programming than the tables. However, to calculate Y_{Fa} and Y_{Sa} by using the equations, the moment arm length (h_{Fa}), rack cutter tip radius (ρ_F) critical tooth thickness (S_{Fn}) should be determined for each tooth number and pressure angle.
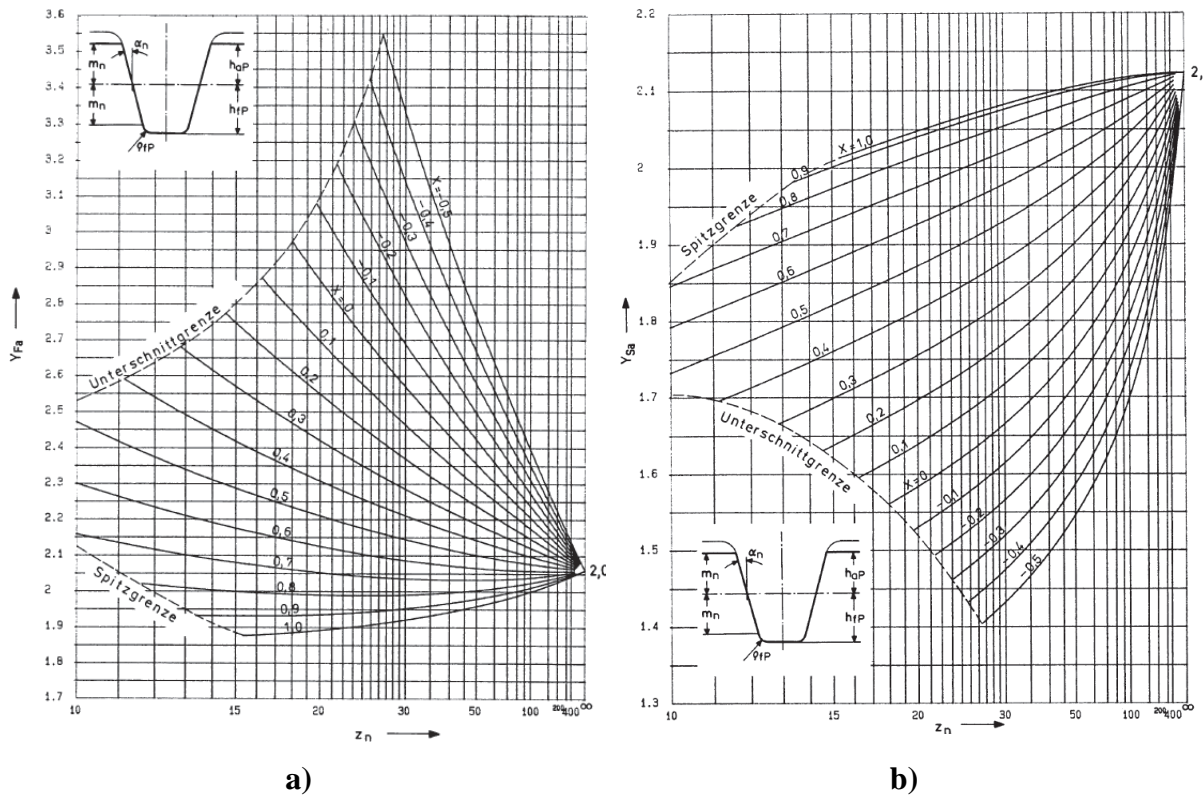
Figure 3. a) The variation of Y_{Fa} (Form factor) **b)** The variation of Y_{Sa} (Stress concentration factor) according to DIN3990 for ρ_F=0.3m (DIN3990, 1987)

2.3. Finite Element Analysis Procedure

Finite element stress analyses were conducted for the determination of the stress distribution of the gears. Moreover, the effects of DSPA and tooth number on the maximum bending stress were investigated numerically. The general finite element stress analysis procedure is divided into five steps as designing the gear geometry, creating the mesh structure, defining the boundary conditions of the analysis, running the analysis, and evaluating the results.

The gear geometries were created according to Litvin's vector method described in Section 2.1. The CAD model was imported to the ANSYS Workbench static structural module for the stress analysis. The mesh structure of the finite element model consisted of approximately 45000 hexahedral (Solid186 and Solid187) elements and 180000 nodes. The general view of the mesh structure of the finite element model is seen in Figure 4.a. A mesh convergence study with different mesh sizes for $20° - 20°$ pressure angle and 20 tooth number were performed. As a result of the convergence, it was observed that there was no significant change in the results after approximately 45000 elements (Figure 4.b).
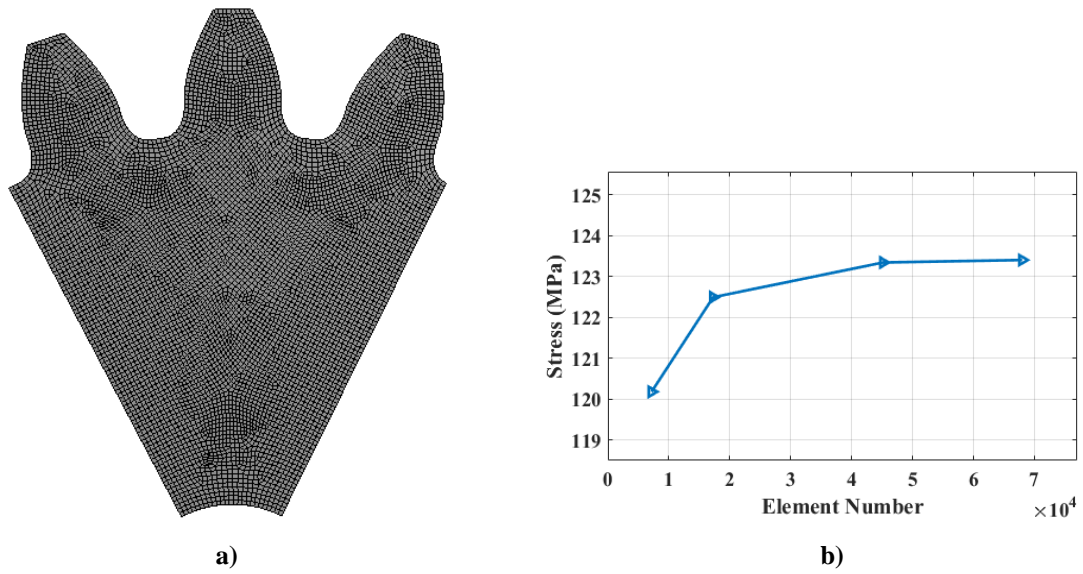
Figure 4. a) Mesh structure of finite element model **b)** Mesh convergence results

After creating the mesh structure of the finite element model, the boundary conditions were defined according to the DIN 3990 / Method C (Figure 5). In this method, a single tooth load applies on the tip of the tooth at the tangent direction of the base circle, as seen in Figure 2. The pressure angle on the addendum circle is calculated by Eq. 7 and the tangential component of the force is calculated by Eq. 8. In the FEA, 100 N static force was applied on the tip of the tooth, and according to the DIN 3990 /Method C standard, the gear geometry was entirely fixed on the side and bottom surfaces.

$$r_0 \cos \alpha = r_a \cos \alpha_a \tag{7}$$

$$F_t = F \cos \alpha_a \tag{8}$$
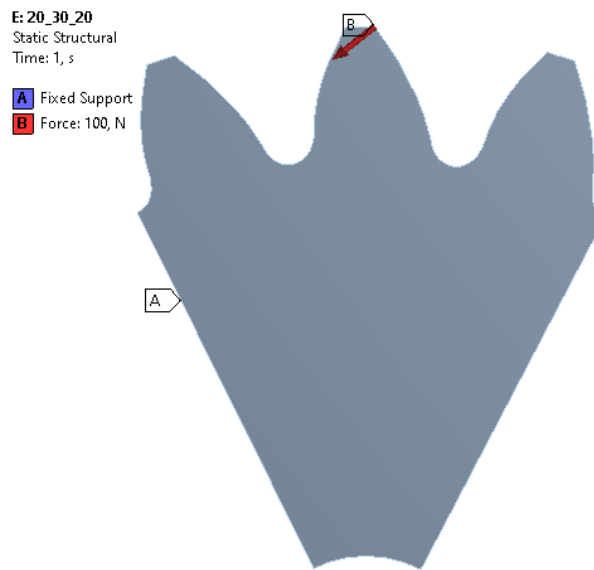
Figure 5. The boundary conditions of the FEA

The main properties of the gear used in this study are given in Table 1. To investigate the effect of DSPA, six different values, 20°, 22°, 24°, 26°, 28° and 30° were determined. For the number of teeth, eleven different values between 18 and 100 were determined. This value was determined as the minimum, since undercut was observed on the spur gears in values below 18 teeth. Moreover, the number of teeth was not increased to avoid the number of analyses since there were not many real samples above 100 teeth.

Table 1. Gear properties of the study

Gear Property	Value
Material	S235 (Steel)
Modulus of elasticity (E) (MPa)	205000
Poisson ratio (v)	0.3
Density (ρ) (kg/m^3)	7850
Module (m) (mm)	3.18
Coast side pressure angle (α_c) (deg)	20
Drive side pressure angle (α_d) (deg)	20-22-24-26-28-30
Tooth number (z)	18-20-23-28-30-35-40-50-70-80-100
Addendum (h_a)	1m
Dedendum (h_f)	1.25m
Face width (b) (mm)	1
Rack cutter tip radius (ρ_F)	0.3m

After the finite element model was created, static structural analysis was performed. The basic finite element equation to be solved for static loads can be expressed as:

$$\{F\} = [K]\{u\} \tag{9}$$

Where F is the applied load vector, K is the stiffness matrix, and u is the displacement vector. Hooke's law was used to calculate the stress distribution of the finite element model. The Hooke's law is written in the following equation.

$$[\sigma] = [E][\varepsilon] \tag{10}$$

3. Results and Discussion

Within the scope of this study, a total of 66 finite element analyzes were carried out for eleven different tooth numbers and six different DSPAs, and maximum bending stresses were examined. Then, the obtained FEA results were compared with the bending stress results calculated by the DIN 3990 method. As an example of the analysis the FEA results for symmetric profile (α_c=20°, α_d=20°) and different tooth numbers (18, 23, 30, 40, 70, and 100) were seen in Figure 6. As can be seen in Table 2, where FEA and analytical method are compared, the results obtained are quite consistent with each other. The maximum

relative error between DIN 3990 and FEA was under 2%. When the bending stresses were investigated for the symmetric case, the stress decreased with the increase in the tooth number. The maximum bending stress values slightly increased when the tooth number increased above 40 and stayed stable according to FEA and DIN 3990.
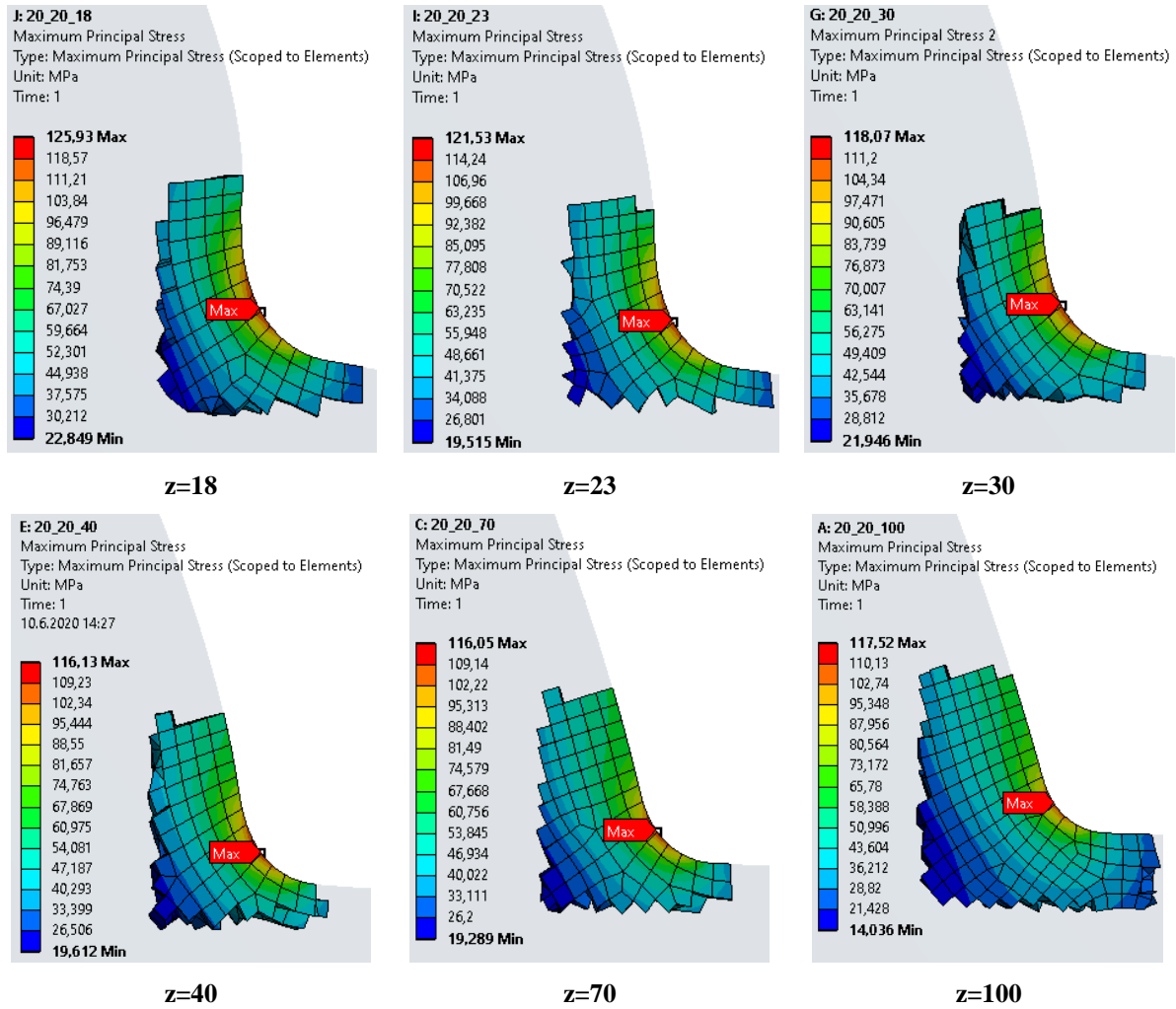
Figure 6. Finite element analysis results for $\alpha_c=20°$, $\alpha_c=20°$, and different tooth numbers

To obtain $Y_{Fa}*Y_{Sa}$ values for a tooth with symmetric profile, maximum bending stresses obtained both from FEA and DIN 3990 norm are normalized using the following equation.

$$Y_{Fa}\, Y_{Sa} = \sigma_{F0-C}\, \frac{b\, m_n}{F_t} \tag{11}$$

Table 2. Comparison of DIN3990 and FEA results of maximum fillet stress for symmetric case (20°-20°)

Z (Teeth Number)	DIN3990 ($\sigma_{F0\text{-}C}$)	FEA ($\sigma_{F0\text{-}C}$)	% Error
18	124.03	125.93	-1.53
20	121.81	123.34	-1.25
23	120.89	121.53	-0.52
28	119.59	118.84	0.62
30	118.89	118.07	0.69
35	116.80	116.84	-0.02
40	117.14	116.13	0.86
50	118.35	116.87	1.25
70	118.11	116.06	1.79
80	118.81	117.17	1.38
100	119.18	117.52	1.39

The variation of $Y_{Fa}*Y_{Sa}$ values depending on the number of teeth was given in Figure 7. The results indicated that both FEA and DIN3990 results were compatible with each other. The value of $Y_{Fa}*Y_{Sa}$ was nearly 4.8 for 18 tooth numbers. The $Y_{Fa}*Y_{Sa}$ value decreased until the tooth number was 40. A small fluctuation was observed in the values obtained with FEA results in the range of 80 to 100 teeth.
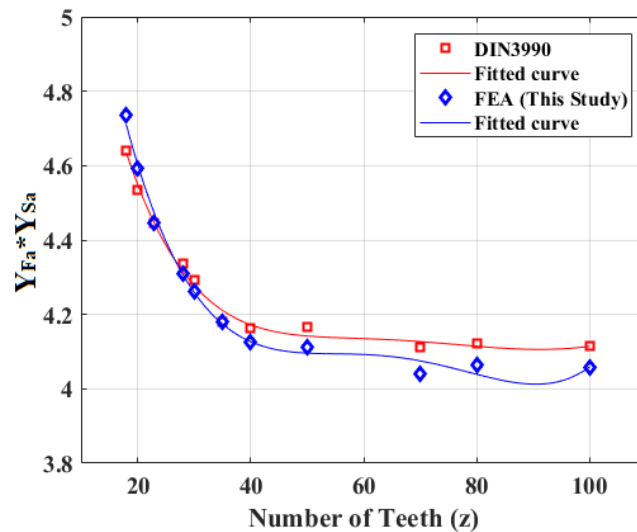
Figure 7. Comparison of $Y_{Fa}*Y_{Sa}$ variation of DIN3990 with finite element analysis

After the maximum bending stresses obtained with the finite element model created for the symmetric tooth profile were verified with the analytical values calculated according to the DIN 3990 standards, this finite element model was started to be used in gears with asymmetric profiles. The FEA results for eleven different tooth numbers and six different DSPA values are given in Table 3. The results showed that DSPA and tooth number have a significant effect on maximum bending stress. When the DSPA

increased, the bending stress was decreased considerably. Approximately the bending stresses were reduced between 20 – 25% depending on the tooth number. The DSPA effect was increased with the increase in the tooth number. The bending stress decreased with the increase in the tooth number nearly until 40.

The main goal of this study was to develop a simplified empirical equation by the DIN 3990 norm using the FEA results to calculate the bending stress of teeth with an asymmetric profile. Accordingly, the normalization process was carried out to obtain a factor called asymmetric factor ($K_{\alpha d}$). The maximum bending stress values obtained with FEA shown in Table 3 were normalized using the following equation.

$$K_{\alpha d} = \frac{\sigma_{F0-C\,(20°-\alpha_d°)}}{\sigma_{F0-C\,(20°-20°)}} \tag{12}$$

where $K_{\alpha d}$ is a new coefficient for calculating asymmetric gear bending stress, $\sigma_{F0-C\,(20°-20°)}$ is the results for symmetric cases and $\sigma_{F0-C(20°-\alpha d°)}$ is the result for asymmetric cases in Table 3.

Table 3. Maximum fillet stress results obtained with FEA (MPa)

		Drive Side Pressure Angle - α_d (°)					
		20	**22**	**24**	**26**	**28**	**30**
	18	125.93	120.69	115.81	110.84	106.01	100.88
	20	123.34	118.38	113.62	108.59	103.29	98.04
	23	121.53	116.15	110.91	105.76	101.03	95.99
	28	118.84	113.38	108.28	103.13	98.59	93.53
Tooth Number (z)	**30**	118.07	112.57	107.27	102.57	97.29	92.27
	35	116.84	111.96	106.90	101.88	95.96	91.40
	40	116.13	111.62	106.06	101.43	94.99	90.83
	50	116.87	111.29	105.73	99.37	94.80	89.74
	70	116.05	111.21	104.31	98.56	93.13	88.56
	80	117.17	110.96	104.40	98.05	93.09	88.06
	100	117.52	110.59	104.06	98.47	93.28	88.44

As a result of normalization depending on different tooth numbers and DSPA are given in Table 4. The results show that both the number of teeth and the DSPA are very important in the asymmetric factor. With increasing DSPA, the asymmetric factor decreased. Furthermore, as a result of the increase in the number of teeth in constant DSPA, there was a decrease in the asymmetric factor again. These results showed that in teeth with asymmetric profiles, root stresses decrease due to the increase in the pressure

angle. The reason can be explained as the thickness in the critical section of the tooth increases, and the stress values decrease with the pressure angle increase.

Table 4. Asymmetric factors ($K_{\alpha d}$) depending on the DSPA and tooth number

		Drive Side Pressure Angle - α_d (°)					
		20	22	24	26	28	30
Tooth Number (z)	18	1	0.958	0.919	0.880	0.841	0.801
	20	1	0.959	0.921	0.880	0.837	0.794
	23	1	0.955	0.912	0.870	0.831	0.789
	28	1	0.954	0.911	0.867	0.829	0.787
	30	1	0.953	0.908	0.868	0.824	0.781
	35	1	0.958	0.914	0.871	0.821	0.782
	40	1	0.961	0.913	0.873	0.817	0.782
	50	1	0.952	0.904	0.850	0.811	0.767
	70	1	0.958	0.898	0.849	0.802	0.763
	80	1	0.947	0.891	0.836	0.794	0.751
	100	1	0.941	0.885	0.837	0.793	0.752

In addition, the variation of the asymmetric factor ($K_{\alpha d}$) depending on the DSPA and the number of teeth is graphically shown in Figure 8. As can be seen from the graph, the increase in DSPA decreased the asymmetric factor, that is, the maximum bending stress in the tooth decreased. The asymmetric factor decreased with the increase in the DSPA value until the number of teeth was 40. According to the obtained results, it is seen that DSPA was more effective than tooth number on the asymmetric factor.
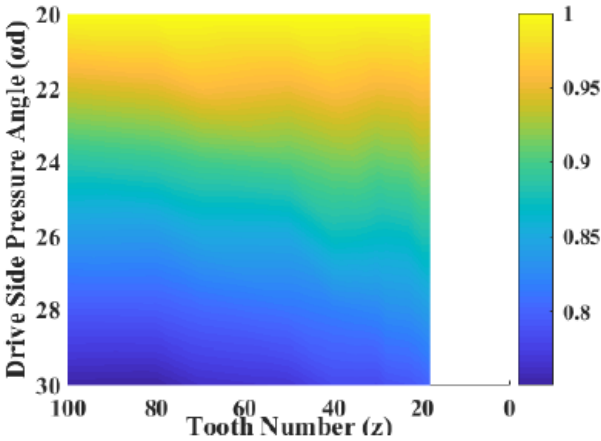
Figure 8. Variation of $K_{\alpha d}$ according to DSPA and tooth number

Since one of the most important purposes of this study is to calculate the bending stress of gears with an asymmetric profile with a simplified equation, the variations in the asymmetric factor ($K_{\alpha d}$) were

investigated. As can be seen from Table 4 and Figure 8, the variation of the asymmetric factor is linear. For this reason, the following equation was used by considering the model to be created in the calculations to be linear.

$$\text{Model} = A\alpha + Bz + C \tag{13}$$

Where α is the DSPA, z is the number of teeth. In this model, the coefficients of A, B and C were calculated by surface fitting and linear regression methods. The determined coefficients of the model were; A= -0.02235, B= -0.0003825 and C= 1.4626. The above equation, in which the asymmetric factor can be calculated depending on the number of teeth and the drive side pressure angle is given below, together with these coefficients.

$$K_{\alpha d} = -0.02235\alpha - 0.0003825z + 1.4626 \tag{14}$$

Including the asymmetric factor ($K_{\alpha d}$) derived in this study into the equation that calculates the bending stress in gears with a symmetric profile according to the DIN 3990 / Method C. With the obtained modified equation, tooth bending stresses can be calculated analytically in asymmetric gears.

$$\sigma_{F0-C} = \frac{F_t}{b \cdot m_n} Y_{Fa} \cdot Y_{Sa} \cdot K_{\alpha d} \tag{15}$$

In this study, tooth bending stresses of asymmetric gears were calculated with the obtained new empirical equation. Firstly, asymmetric factors ($K_{\alpha d}$) were calculated for six different DSPAs and eleven different tooth numbers. Then, the obtained ($K_{\alpha d}$) was used in the above equation. The maximum bending stresses calculated with the modified empirical equation depending on the different pressure angles and the number of teeth are given in Table 5. As well as, to determine the accuracy of the empirical model developed in this study, the stress values obtained with the empirical equation were compared with the results of the finite element analysis in Figure 9. It was observed that there is a great agreement between the maximum bending stress values obtained using the modified empirical formula and the stresses obtained as a result of FEA. The maximum relative error was detected as 2.4% and the average relative error was around 1%. These results show that the new empirical equation obtained with the method followed in the study gives very sensitive results. By using this new equation, bending stresses of asymmetric gears can be calculated analytically without the need for finite element analysis.

Table 5. Maximum fillet stress results obtained with novel equation

		Drive Side Pressure Angle - α_d (°)					
		20	**22**	**24**	**26**	**28**	**30**
Tooth Number (z)	**18**	124.03	118.82	113.98	109.15	104.31	99.35
	20	121.81	116.82	112.19	107.19	101.95	96.72
	23	120.89	115.45	110.25	105.17	100.46	95.38
	28	119.59	114.09	108.95	103.68	99.14	94.12
	30	118.89	113.30	107.95	103.20	97.97	92.85
	35	116.80	111.89	106.76	101.73	95.89	91.34
	40	117.14	112.57	106.95	102.26	95.70	91.60
	50	118.35	112.67	106.99	100.60	95.98	90.77
	70	118.11	113.15	106.06	100.28	94.72	90.12
	80	118.81	112.51	105.86	99.33	94.34	89.23
	100	119.18	112.15	105.47	99.75	94.51	89.62
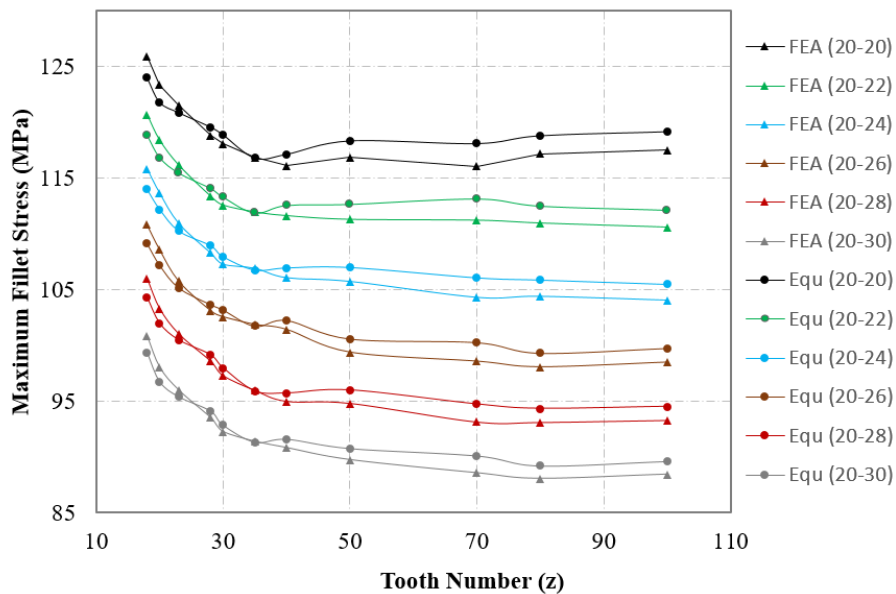
Figure 9. Comparison of maximum fillet stress results obtained with FEA and empirical equation

4. Conclusions

In this study, a simplified empirical equation has been developed to analytically calculate the maximum bending stress for gears with asymmetrical tooth profile, which is widely used in many critical sectors such as defense, energy and aerospace. While there are analytical methods determined by ISO 6336-1:2019, ANSI/AGMA 2001-D04 and DIN 3990 norms in the literature to calculate the maximum bending stresses of gears with symmetrical profile, there is no standard for asymmetric gears. In this

study, maximum bending stresses of asymmetric teeth were calculated for six different drive side pressure angles and eleven different tooth numbers using the FE model validated on the symmetrical tooth. With the normalization of the stress results obtained from the FEA, the factor called asymmetric factor ($K_{\alpha d}$) was obtained. After the linear model was created, asymmetric factors were calculated depending on the DSPA and the number of teeth. The empirical equation used to calculate the stresses in the symmetrical gears in the DIN 3990 / Method C was modified by adding an asymmetric factor. In order to determine the accuracy of the empirical model developed in this study, the stress values obtained with the empirical equation were compared with the results of the FEA. It was observed that there is a great agreement between the maximum bending stress values obtained using the modified empirical formula and the stresses obtained as a result of FEA. The maximum relative error was detected as 2.4% and the average relative error was around 1%. Thanks to the empirical equation obtained, it has been seen that the bending stresses of asymmetric gears can be calculated with high accuracy without the need for finite element analysis.

4. Future Work

The gears used in this study have the standard design specified in Table 1. Therefore, the equation obtained as a result of the study is valid only for this design set. The effect of different rack cutters on the equation will be investigated after this study.

NOMENCLATURE

α : Pressure angle

α_d : Standard pressure angle – 20°

a_d : Distance between axis

b : Face width

ε_α : Contact ratio

F : Applied single force

F_T : Tangential gear force

$K_{\alpha d}$: Asymmetry factor

h_a : Addendum

h_f : Dedendum

h_{Fa} : Moment arm length

m/m_n : Module

r_{a1} : Addendum circle of the pinion

r_{a2} : Addendum circle of the gear

r_{b1} : Base circle of the pinion

r_{b2} : Base circle of the gear

σ_{F0-C} : Maximum tooth root stress

p	: Pitch
ρ_F	: Rack cutter tip radius
s_{Fn}	: Critical tooth thickness
x	: Profile shifting
Y_{Fa}	: Form factor
Y_{Sa}	: Stress correction factor
Y_ε	: Load sharing factor
Y_β	: Helis factor
r_0	: Pitch circle
z	: Tooth number

Conflict of Interests

We confirm that there are no conflicts of interest related to this publication, and no significant financial support has been received for this work that could have impacted its outcomes.

Authors' contributions

OD (35%), and CY (35%) generated the finite element model. OD, CY and FK (30%) compared and interpreted analysis results with analytical solutions. All authors read and approved the final manuscript.

References

Cavdar K., Karpat F., Babalik FC. Computer aided analysis of bending strength of involute spur gears with asymmetric profile. Journal of Mechanical Design 2005; 127: 477-484.

Costopoulos TN., Spitas CA. Optimum gear tooth geometry for minimum fillet stress using BEM and experimental verification with photoelasticity. Journal of Mechanical Design 2016; 128(5): 1159-1164.

Costopoulos TN., Spitas V. Reduction of gear fillet stresses by using one-sided involute asymmetric teeth, Mechanism and Machine Theory 2009; 44: 1524-1534.

Demet SM., Ersoyoğlu AS. Fatigue fracture behaviour of asymmetric spur gear tooth under cyclic loading. Procedia Structural Integrity 2018; 13: 2030-2035.

Dharashivkar NS., Sondur VB., Joshi KD. 3D photoelastic and finite element analysis of asymmetric involute spur gear. International Conference on Electrical, Electronics, and Optimization Techniques ICEEOT 2016; 1838-1842.

DIN3990. Calculation of load capacity of cylindrical gears: Calculation of tooth strength. 1987.

Dogan O., Yılmaz TG. Karpat F. Stress analysis of involute spur gears with different parameters by finite element and graphical method. Journal of the Faculty of Engineering and Architecture of Gazi University 2018; 33:1493-1504.

Drago RJ. An Improvement in the conventional analysis of gear tooth bending fatigue strength. American Gear Manufacturers Association 1982; 229-224.

Francesco GD., Marini S. Asymmetric teeth: Bending stress calculation, Gear Technology 2007; 24: 52-55.

He R., Tenberge P., Xu X., Li H., Uelpenich R., Dong P., Wang S. Study on the optimum standard parameters of hob optimization for reducing gear tooth root stress. Mechanism and Machine Theory 2021; 104128.

ISO 6336 – Calculation of load capacity of spur and helical gears - Application for industrial gears, 2002.

Kalay OC., Dogan O., Yılmaz TG. Yuce C., Karpat F. A comparative experimental study on the impact strength of standard and asymmetric involute spur gears. Measurement 2020; 172: 108950.

Kapelevich A. Geometry and design of involute spur gears with asymmetric teeth. Mechanism and Machine Theory 2000; 35: 117-130.

Karpat F., Cavdar K., Babalik FC. Computer aided analysis of involute spur gears with asymmetric teeth. VDI Berichte 2005; 145-163.

Karpat F., Dogan O., Ekwaro-Osire S., Yuce C. A novel method for calculation gear tooth stiffness for dynamic analysis of spur gears with asymmetric teeth. ASME International Mechanical Engineering Congress & Exposition 2014; 1-8.

Karpat F., Ekwaro-Osire S., Cavdar K., Babalik FC. Dynamic analysis of involute spur gears with asymmetric teeth. International Journal of Mechanical Sciences 2008; 50: 1598-1610.

Karpat F., Yuce C., Dogan O. Experimental measurement and numerical validation of single tooth stiffness for involute spur gears. Measurement 2020; 150: 107043.

Keçici A., Ünüvar A. Investigation of the effect of pressure angle on gear performance in asymmetric gears. Meccanica 2021; 56: 2919-2933.

Kumar VS., Muni V., Muthuveerappan G. Optimization of asymmetric spur gear drives to improve the bending load capacity. Mechanism and Machine Theory 2008; 43: 829-858.

Lisle TJ., Shaw BA. Frazer, RC. Frazer. External spur gear root bending stress: A comparison of ISO 6336: 2006, AGMA 2101-D04, ANSYS finite element analysis and strain gauge techniques. Mechanism and Machine Theory 2017; 111: 1-9.

Litvin FL., Lian Q., Kapelevich A. Asymmetric modified spur gear drives: Reduction of noise, localization of contact, simulation of meshing and stress analysis. Computer Methods in Applied Mechanics and Engineering 2000; 188: 363-390.

Marimuthu P., Muthuveerappan G. Investigation of load carrying capacity of asymmetric high contact ratio spur gear based on load sharing using direct gear design approach. Mechanism and Machine Theory 2016; 96: 52-74.

Pedersen NL. Improving bending stress in spur gears using asymmetric gears and shape optimization. Mechanism and Machine Theory 2010; 45: 1707-1720.

Pramono AS., Rizal MZ. Influence of asymmetric factor on spur gears to dynamic bending stress. IOP Conf. Series: Materials Science and Engineering 2021; 1034: 012010.

Sekar RP., Muthuveerappan G. Estimation of tooth form factor for normal contact ratio asymmetric spur gear tooth. Mechanism and Machine Theory 2015; 90: 187-218.

Spitas V., Spitas C. Optimizing involute gear design for maximum bending strength and equivalent pitting resistance. Proceedings of the Institution of Mechanical Engineers, Part C: Journal of Mechanical Engineering Science 2007; 221: 479-488.

Thomas B., Sankaranarayanasamy K., Ramachandra S., Kumar SPS. Search method applied for gear tooth bending stress prediction in normal contact ratio asymmetric spur gears. Proceedings of the Institution of Mechanical Engineers, Part C: Journal of Mechanical Engineering Science 2018; 232: 4647-4663.

Yılmaz TG., Karadere G., Karpat F. A numerical analysis of hybrid spur gears with asymmetric teeth: stress and dynamic behavior. Machines 2022; 10(11): 1056.

Wen Q., Du Q., Zhai X. A new analytical model to calculate the maximum tooth root stress and critical section location of spur gear. Mechanism and Machine Theory 2018; 128: 275-286.